Trabalho apresentado no XXXIX CNMAC, Uberlândia - MG, 2019.

Proceeding Series of the Brazilian Society of Computational and Applied Mathematics

Diffusive Riemann Solutions for 3-phase flow in Porous Media

Luis Fernando Lozano Guerrero [1]
Dep. de Matemática, Universidade Federal de Juiz de Fora
Dan Marchesin [2]
Instituto Nacional de Matematica Pura e Aplicada, IMPA

Abstract. We study the diffusive effect caused by capillary pressure in three-phase flow in porous media, which is modeled by a system of two nonlinear conservation laws. We solve a class of Riemann problems where one of the viscosities is higher than the other two; we first develop a methodology using artificial diffusion and identify the transitional surfaces and associated shocks, resulting from loss of strict hyperbolicity at an isolated point in the space of saturations. We identify the surfaces that characterize solutions which require transitional shocks. We use the wave curve method to determine the solutions for arbitrary Riemann data, except for a small set of right states that utilize transitional rarefactions. We present the transitional surface for the general case where diffusion arises from capillary effects.

Key words. Flows in porous media, capillary pressure, viscous profiles, conservation laws.

1 Introduction

Here, we solve a now longstanding unresolved problem in shock wave theory, namely, to characterize the nonlinear wave structure that emerges from discontinuous (Riemann) initial data for the problem of three phase flow in a porous medium. The wave structure is described for most pairs of constant states, and a precise notion of uniqueness and continuous dependence on initial states is formulated and demonstrated to apply.

The main obstacle to a characterization of nonlinear waves in three-phase flow is the presence of umbilic points where wave speeds coincide. This leads to the presence of complicated waves that obscure the recognition of stable wave structures from unstable ones. We give the solution to the Riemann problem for the equations of three-phase flow, including a successful entropy condition for choosing the stable family of solutions, and providing compelling evidence that such a family exists having the property of continuous dependence on left and right states.

We now describe briefly previous work related to our study, see [13] for details. In [8, 9], Isaacson *et. al.* identified transitional waves in the Riemann solution of certain pairs of conservation laws. Unlike classical shocks, for transitional shocks, the Rankine-Hugoniot constraints linking the states on the sides of the shock are insufficient to determine the

[1] luisfer99@gmail.com
[2] marchesi@impa.br

DOI: 10.5540/03.2020.007.01.0372

waves emerging along outgoing characteristics. It was shown in [11, 12] that the requirement of existence of viscous profiles gives the right number of additional constraints. Also, the additional equations resulting from the viscous profile requirement are introduced explicitly. In [6, 7], Azevedo *et. al.* established existence, uniqueness and L^1_{loc}-continuity under change of data of Riemann solutions for green reservoirs. In [3] Andrade *et. al.* exhibited Riemann solutions for right states near vertex O and left states along $[G, W]$. In [4] the results were extended for right states near O. In [5], in the presence of nontrivial diffusion terms, it is not the elliptic region that plays the role of an instability region; rather, it is the region defined by Majda-Pego. In [1, 2], Abreu *et. al.*, performed two dimensional numerical simulations of Riemann solutions with capillary effects.

This work is organized as follows. In Section 2, we recall the mathematical model for three-phase flow in porous media and discuss the admissibility of discontinuities under the viscous profile criterion. In Section 3 construct the backward fast wave curves and the so-called $\mathscr{R}$-regions associated with them. In Section 4 we determine the $\mathscr{L}$-regions associated to some $\mathscr{R}$-region described in Section 3. In Section 5 we present the surface of transitional shocks for a physically correct viscosity matrix.

Our numerical experiments used the softwares "RPN" and "ELI," developed in close collaboration with B. J. Plohr. Calculations in MATLAB were also performed.

2 Mathematical model

In this section, we recall some basic facts about the mathematical model, which is also studied in [6, 7, 9]. We consider the flow of a mixture of three fluid phases (water, gas and oil) in a thin, horizontal cylinder of porous rock. Let $s_{\mathrm{w}}(x,t)$, $s_{\mathrm{g}}(x,t)$ and $s_{\mathrm{o}}(x,t)$ denote the corresponding saturations at distance x along the cylinder, at time t. Under our simplifications, the governing equations for three-phase flow become

$$\partial_t s_{\mathrm{w}} + \partial_x f_{\mathrm{w}} = 0, \quad \partial_t s_{\mathrm{o}} + \partial_x f_{\mathrm{o}} = 0, \tag{1}$$

which is a non-dimensionalized system representing conservation of water, gas, oil, and Darcy's law. We adopt the following flux functions:

$$f_{\mathrm{w}} = s_{\mathrm{w}}^2/(\mu_{\mathrm{w}}\mathscr{D}), \qquad f_{\mathrm{o}} = s_{\mathrm{o}}^2/(\mu_{\mathrm{o}}\mathscr{D}), \text{ where } \mathscr{D} = s_{\mathrm{w}}^2/\mu_{\mathrm{w}} + s_{\mathrm{o}}^2/\mu_{\mathrm{o}} + s_{\mathrm{g}}^2/\mu_{\mathrm{g}} > 0, \tag{2}$$

and the constants μ_{w}, μ_{o} and μ_{g} are the phase viscosities. These represent a simple Corey's model with quadratic relative permeability functions. Because $s_{\mathrm{w}} + s_{\mathrm{g}} + s_{\mathrm{o}} = 1$ and $0 \le s_{\mathrm{w}}, s_{\mathrm{o}}, s_{\mathrm{g}} \le 1$, following practice in petroleum engineering we depict the space of states of the fluid mixture in barycentric coordinates as the saturation triangle shown in Fig. 1, where we use the labels O, W, and G to designate the states with saturation $s_{\mathrm{o}} = 1$, $s_{\mathrm{w}} = 1$, and $s_{\mathrm{g}} = 1$, respectively. The state B corresponds to $s_{\mathrm{o}} = 0$, $s_{\mathrm{w}} = \mu_{\mathrm{w}}/(\mu_{\mathrm{w}} + \mu_{\mathrm{g}})$, and $s_{\mathrm{g}} = \mu_{\mathrm{g}}/(\mu_{\mathrm{w}} + \mu_{\mathrm{g}})$; the state D to $s_{\mathrm{o}} = \mu_{\mathrm{o}}/(\mu_{\mathrm{w}} + \mu_{\mathrm{o}})$, $s_{\mathrm{w}} = \mu_{\mathrm{w}}/(\mu_{\mathrm{w}} + \mu_{\mathrm{o}})$, and $s_{\mathrm{g}} = 0$; the state E to $s_{\mathrm{o}} = \mu_{\mathrm{o}}/(\mu_{\mathrm{g}} + \mu_{\mathrm{o}})$, $s_{\mathrm{w}} = 0$, and $s_{\mathrm{g}} = \mu_{\mathrm{g}}/(\mu_{\mathrm{g}} + \mu_{\mathrm{o}})$. The state $\mathcal{U}$ in Fig. 1 is an umbilic point [14]. It is the unique state in the interior of the saturation triangle where the characteristic speeds coincide; its coordinates are determined by the fluid viscosities as $s_{\mathrm{o}} = \mu_{\mathrm{o}}/\mu_{\mathrm{tot}}$, $s_{\mathrm{w}} = \mu_{\mathrm{w}}/\mu_{\mathrm{tot}}$, and $s_{\mathrm{g}} = \mu_{\mathrm{g}}/\mu_{\mathrm{tot}}$, with $\mu_{\mathrm{tot}} = \mu_{\mathrm{w}} + \mu_{\mathrm{o}} + \mu_{\mathrm{g}}$.

DOI: 10.5540/03.2020.007.01.0372

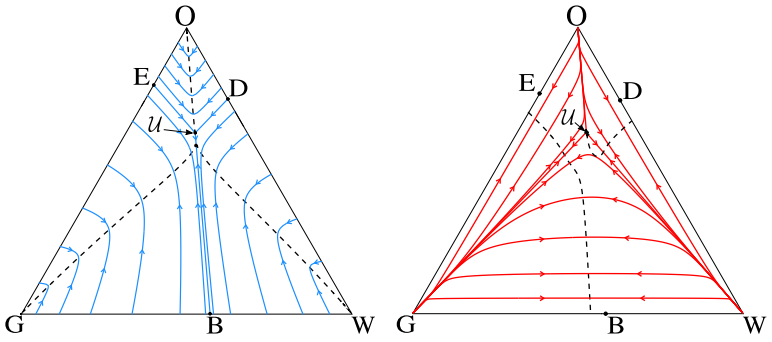

(a) Slow-family integral curves. (b) Fast-family integral curves.

Figure 1: Integral curves for characteristic families. The arrow indicates the direction on which characteristic speeds increase. The inflection curves for each family are represented by dashed lines. In this figures the umbilic point is of type II_O.

2.1 Admissibility of discontinuities

In multiphase flow, it is essential to take into account the effect of capillary pressure between the different fluids. Instead of the system (1), we obtain the following parabolic system:

$$U_t + F(U)_x = \epsilon \left(\mathcal{B}(U)U_x\right)_x . \tag{3}$$

Of course the original equations were properly scaled, and the coefficient ϵ of the diffusive term in (3) is often rather small. In this system $U = (s_{\mathrm{w}}, s_{\mathrm{o}})^T, F(U) = (f_{\mathrm{w}}(U), f_{\mathrm{o}}(U))^T$, and $\mathcal{B}(U)$ is a matrix depending on the relative permeabilities and viscosities of the three fluids, and on the partial derivatives of capillary pressures, see Chapter 3 of [10]. In [5], it is shown that $\mathcal{B}(U)$ is symmetric and positive definite in the interior of the saturation triangle. In view of system (3), the natural admissibility criterion for shocks is the viscous profile criterion: a shock joining U^- to U^+ must be the limit, as the positive parameter ϵ tends to zero, of traveling wave solutions $U(x,t) = \widetilde{U}((x-\sigma t)/\epsilon)$ of the parabolic system (3), where $\sigma = \sigma(U^-, U^+)$ is the shock speed, with the boundary conditions $U(-\infty) = U^-$ and $U(+\infty) = U^+$. Since the traveling wave U is a smooth function of $\xi = (x-\sigma t)/\epsilon$, this system can be integrated to yield the system of ordinary differential equations

$$\mathcal{B}(U(\xi))\, U'(\xi) = -\sigma \left(U(\xi) - U^-\right) + F(U(\xi)) - F(U^-), \tag{4}$$

for which both U^- and U^+ are singularities of the vector field. A traveling wave solution corresponds to a connection U^- to U^+ and is called a viscous profile of the shock wave.

3 Wave curves

Now, we characterize the wave curves in the Corey Quad model with $\mathcal{B}(U) = I$. Since we want to use the wave curves to solve the Riemann problem in the whole saturation triangle for $\mathcal{U}$ of type II, we first identify the regions where the wave curves have the same number and types of waves groups. Then, we study how these regions change when

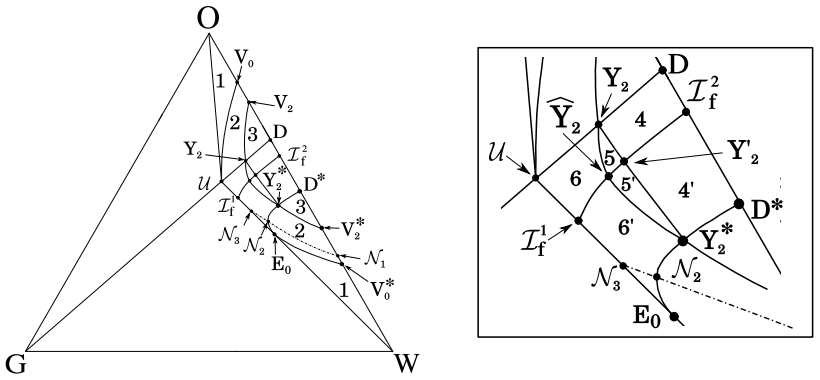

(a) Regions $\mathscr{R}_1, \mathscr{R}_2$ and $\mathscr{R}_3$.

(b) Highlight of regions $\mathscr{R}_i$ for $i \in \{4, 4', 5, 5', 6, 6'\}$.

Figure 2: Subdivisions of subtriangle $\{O,\mathcal{U},W\}$ in $\mathscr{R}$-regions for $1 < \mu_{\rm w}+\mu_{\rm o}/\mu_{\rm g} < 8$ and $\mathcal{U} \in II_O$.

μ_w, μ_o and μ_g vary. These results provide scientific evidence for the existence of Riemann solutions, based on a combination of analytical and computational techniques.

3.1 Subdivision in backward $\mathscr{R}$-regions: umbilic point type II

Let T be an open set of states in the saturation triangle. We say that T is a backward (alternatively, a forward) $\mathscr{R}$-region if for every right state $R \in T$, the backward (forward) fast wave curve $\mathcal{W}_f^-(R)$ $(\mathcal{W}_f^+(R))$, has the same structure, *i.e*, it has exactly the same wave sequence. We define forward (backward) $\mathscr{L}$-regions similarly.

The methodology for constructing of the $\mathscr{R}$-regions is as follows: first, we find the bifurcation manifolds (Chapter 4 of [10]) and the boundaries for compatibility and admissibility loss (Section 6.2 of [10]). We also consider the extensions of segments of the invariant line associated to the subtriangle $\{O,\mathcal{U},W\}$. Then, we build the backward fast wave curves in $\{O,\mathcal{U},W\}$ using the succession algorithm from Section (2.7) of [10], studying the behavior of each wave group with respect to the bifurcation manifolds and the compatibility boundaries, and verifying numerically if each Lax f-shock has viscous profile.

We restrict this presentation to the the subtriangle $\{O,\mathcal{U},W\}$. We study the case with umbilic point $\mathcal{U} \in II_O$, where $\mu_{\rm o} + \mu_{\rm g}/\mu_{\rm w} > 1$, $\mu_{\rm w} + \mu_{\rm g}/\mu_{\rm o} < 1$ and $1 < \mu_{\rm w} + \mu_{\rm o}/\mu_{\rm g} \leq 8$. In Figure (2) we show the subdivision in $\mathscr{R}$-regions for the subtriangle $\{O,\mathcal{U},W\}$. The description of the curves that define each region and the other cases can be found in [10].

4 Diagrams of comparison between regions

In this section, we summarize the distinct Riemann solutions and study the behavior of these solutions in two types of data variation. In the first setting, we fix the right state R and see how solutions change continuously as L traverses the phase space continuously. Notice how the bifurcations and the compatibility boundaries take the role of transition bridges between regions. In the second variation scenario, by fixing L and varying R

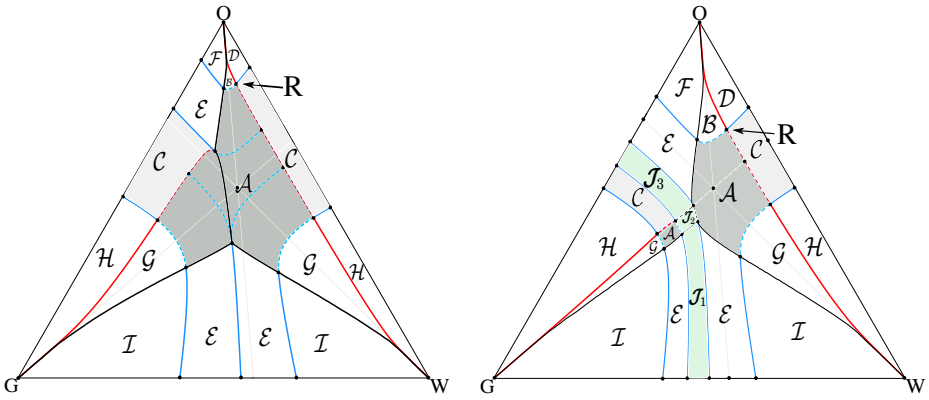

(a) $\mathscr{L}$-regions for R in region $\mathscr{R}_1$. (b) $\mathscr{L}$-regions for R in region $\mathscr{R}_2$.

Figure 3: Diagrams of changes between $\mathscr{L}$-regions for R in region $\mathscr{R}_1$ and $\mathscr{R}_2$, see Figure 2. Green region represents the left states L that use single transitional shocks in the Riemann solution. The nomenclature for structures $\mathcal{A}, \mathcal{B}, \ldots, \mathcal{I}, \mathcal{J}_1, \mathcal{J}_2$ and $\mathcal{J}_3$ are in Table 1.

continuously, we can see how $\mathscr{L}$-regions arise or disappear continuously. There is a third possible variation study to analyze the behavior of Riemann solutions: when we vary the viscosities (while keeping the umbilic point of type II) the boundaries of the $\mathscr{R}$-regions move. So, even with the right state R fixed, it changes regions continuously in a similar manner to the first variation setting. In Table 1 we summarize the possible solutions that

$\mathcal{A}:\ S_s\,S_f$	$\mathcal{B}:\ S_s\,R_f$	$\mathcal{C}:\ R_s\,S_f$	$\mathcal{D}:\ R_s\,R_f$
$\mathcal{E}:\ R_s\,'S_s\,S_f$	$\mathcal{F}:\ R_s\,'S_s\,R_f$	$\mathcal{G}:\ S_s\,R_f\,'S_f$	$\mathcal{H}:\ R_s\,R_f\,'S_f$
$\mathcal{I}:\ R_s\,'S_s\,R_f\,'S_f$	$\mathcal{J}_1:\ R_s\,'S_s\,S_T\,S_f$	$\mathcal{J}_2:\ S_s\,S_T\,S_f$	$\mathcal{J}_3:\ R_s\,S_T\,S_f$

Table 1: Nomenclature of distinct waves structures in $\mathscr{L}$-regions for the $\mathscr{R}_1$ and $\mathscr{R}_2$-regions.

are involved in classical and transitional Riemann solutions, not considering the delta wing [10] and transitional rarefactions. The justification and description of the $\mathscr{L}$ and $\mathscr{R}$-regions can be found in [10]. Notice that the number of different structures varies as we change the $\mathscr{R}$-region. For example, if considering $R \in \mathscr{R}_1$, we have only nine distinct structures, see Figure 3(a). Transitional waves are not used in this case. In Figure (3)(b) we show the division in $\mathscr{L}$-regions for R into the $\mathscr{R}_2$-region which use transitional shocks.

5 Nonlinear effects of capillarity induced diffusion

In Figure 4 we present the surface of transitional shocks for the case $\mathcal{B}(U) \neq I$ which was constructed numerically. We consider the general case with $\mathcal{B}(U)$ defined in Chapter 3 of [10]. This matrix is associated with the correct diffusive effects caused by capillary pressures [1, 2, 5]. We show that the surface of transitional shocks for this case has the same topological structure found in the case of $\mathcal{B}(U) = I$, see Chapter 7 [10].

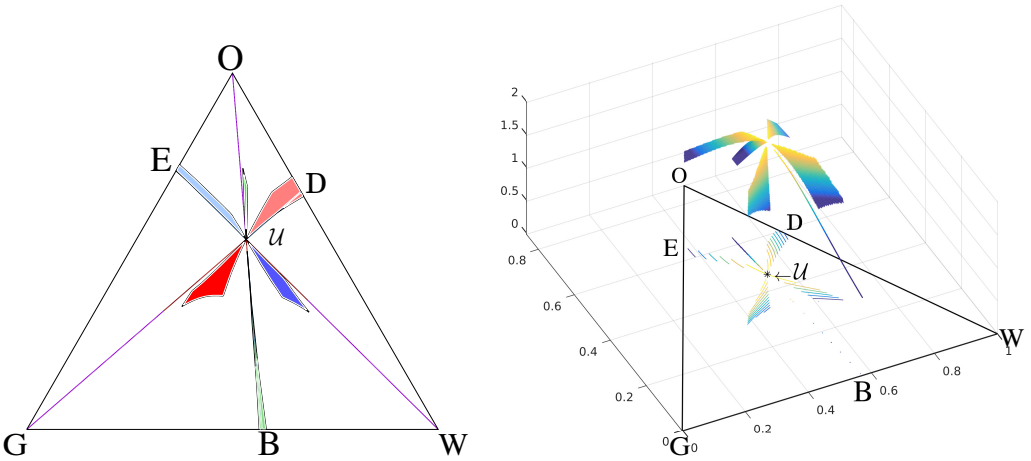

(a) Projection of the surface of transitional shocks in the saturation triangle.

(b) Surfaces of transitional shocks for $[G, D], [W, E]$ and $[O, B]$ in $3D$ phase space.

Figure 4: Surfaces of transitional shocks for umbilic point of type II_O and $\mathcal{B}(U) \neq I$.

6 Conclusions

Here is a summary of our contributions to the problem of three-phase flow in porous media, taking the viscosity matrix to be a multiple of the identity, and for arbitrary fluid viscosities placing the umbilic point in case II of the Schaeffer-Shearer classification.

We characterized the structurally stable Riemann solutions. Namely, we determined the sets of Riemann problems whose solutions have the same wave structure, in terms of number, type and sequence of elementary waves. In the process, we studied the bifurcations of backward-fast and forward-slow wave curves. This study led to the understanding of how the saturation triangle is subdivided, depending on viscosity values, into $\mathscr{R}$-regions of right Riemann states for which the backward-fast wave curves are structurally stable. This subdivision, in turn, induces a subsequent subdivision of the saturation triangle, for each $\mathscr{R}$-region, into $\mathscr{L}$-regions of left Riemann states for which the corresponding Riemann solutions are structurally stable. We presented the complete solution to the Riemann problem for three-phase flow. This includes demonstrating a successful entropy condition for choosing the stable family of solutions, and establishing the compelling result that such a family exists having the property of continuous dependence on left and right states. We have also constructed the surface of transitional shocks for the general case of nonlinear viscosity matrices resulting from correct capillarity induced diffusive effects. Many suggestions from F. Furtado, A. de Souza and B. J. Plohr are gratefully acknowledged.

References

[1] E. Abreu, J. Douglas, F.Furtado, D. Marchesin, and F. Pereira. Three-phase immiscible displacement in heterogeneous petroleum reservoirs, *Mathematics and Computers in Simulation*, 73:2-20, 2006. DOI:10.1016/j.matcom.2006.06.018.

[2] E. Abreu. Numerical modelling of three-phase immiscible flow in heterogeneous porous media with gravitational effects, *Mathematics and Computers in Simulation*, 97:234-259, 2014. DOI:10.1016/j.matcom.2013.09.010.

[3] P. Andrade, A. de Souza, F. Furtado, and D. Marchesin. Oil displacement by water and gas in a porous medium: the Riemann problem. *Bull. Braz. Math. Soc. (N.S.)*, 47(1):1–14, 2016. DOI:10.1007/s00574-016-0123-4.

[4] P. Andrade, A. de Souza, F. Furtado, and D. Marchesin. Three-phase fluid displacement in a porous medium. *Journal of Hyperbolic Differential Equations*, 15(4):731–753, 2018. DOI:10.1142/S0219891618500236.

[5] A. Azevedo, D. Marchesin, B. Plohr, and K. Zumbrun. Capillary instability in models for three-phase flow. *Zeitschrift fur Angewandte Mathematik und Physik*, 53(5):713–746, 2002. DOI:10.1007/s00033-002-8180-5.

[6] A. Azevedo, A. de Souza, F. Furtado, D. Marchesin, and B. Plohr. The solution by the wave curve method of three-phase flow in virgin reservoirs. *Transport in Porous Media*, 83(1):99–125, 2010. DOI:10.1007/s11242-009-9508-9.

[7] A. Azevedo, A. de Souza, F. Furtado, and D. Marchesin. Uniqueness of the Riemann solution for three-phase flow in a porous medium. *SIAM J. Appl. Math.*, 74(6):1967–1997, 2014. DOI:10.1137/140954623.

[8] E. Isaacson, D. Marchesin, and B. Plohr. Transitional waves for conservation laws. *SIAM J. Math. Anal.*, 21(4):837–866, 1990. DOI:10.1137/0521047

[9] E. Isaacson, D. Marchesin, B. Plohr, and B. Temple. Multiphase flow models with singular Riemann problems. *Comput. Appl. Math.*, 11(2):147–166, 1992.

[10] L. Lozano. Diffusive effects in Riemann solutions for the three phase flow in porous media. PhD thesis, Instituto Nacional de Matemática Pura e Aplicada, IMPA, 2018.

[11] D. Marchesin and A. A. Mailybaev. Dual-family viscous shock waves in systems of conservation laws: a surprising example. *In Proc. Conf. on Analysis, Modeling and Computation of PDE and Multiphase Flow*. Stony Brook NY, 2004.

[12] D. Marchesin and A. A. Mailybaev. Dual-family viscous shock waves in n conservation laws with application to multi-phase flow in porous media. *Arch. Rational Mech. Anal.*, 182(1):1–24, 2006. DOI:10.1007/s00205-005-0419-9.

[13] D. Marchesin and B. Plohr. Wave Structure in WAG Recovery. *Society of Petroleum Engineers*, 6(2):209–219, 2001. DOI:10.2118/71314-PA

[14] M. Shearer, D. G. Schaeffer, D. Marchesin, and P. L. Paes-Leme. Solution of the Riemann problem for a prototype 2 X 2 system of nonstrictly hyperbolic conservation laws. *Arch. Rational Mech. Anal.*, 97(4):299–320, 1987. DOI:10.1007/BF00280409

